sustainability

MDPI

Article

Crowd Evacuation through Crossing Configurations: Effect of Crossing Angles and Walking Speeds on Speed Variation and Evacuation Time

Shabna SayedMohammed [1], Anshi Verma [1], Charitha Dias [1,2,*], Wael Alhajyaseen [1,2], Abdulkarim Almukdad [2] and Kayvan Aghabayk [3]

1 Department of Civil & Architectural Engineering, College of Engineering, Qatar University, Doha P.O. Box 2713, Qatar
2 Qatar Transportation and Traffic Safety Center, College of Engineering, Qatar University, Doha P.O. Box 2713, Qatar
3 School of Civil Engineering, College of Engineering, University of Tehran, Tehran 111554563, Iran
* Correspondence: cdias@qu.edu.qa

Abstract: The design of safe and efficient pedestrian facilities necessitates the knowledge of complex human movements, such as intersecting pedestrian streams, under different conditions. This study aims to experimentally investigate the impact of intersecting angles on collective crowd dynamics under two different urgency levels. Data were collected from a controlled laboratory experiment with scenarios consisting of three intersection angles (30°, 90°, and 150°) and two desired speed levels (normal walking and slow running). Trajectory data of individual experiment participants were extracted from the recorded video footage. The results indicate that the 30° intersection has the lowest bottleneck effect compared to the other angles. Moreover, the time-to-target analysis shows that the 150° intersection has a higher waiting time at the intersection compared to the other angles for the jogging scenarios. The speed distribution and space utilization maps implied an asymmetrical reduction in speed in the two corridors of the intersection, even though the physical and geometrical configurations are symmetric. The lane-based analysis of collective speeds revealed that the inner lane (the lane that initially encounters the intersecting flow) has the maximum reduction in speed. The outcomes of this study may be useful to evaluate the congestion effects associated with crossing configurations and in calibrating and validating simulation tools to reproduce such effects accurately.

Keywords: pedestrian flow; crossing flows; walking speed; speed variation; crowd dynamics; evacuation

Citation: SayedMohammed, S.; Verma, A.; Dias, C.; Alhajyaseen, W.; Almukdad, A.; Aghabayk, K. Crowd Evacuation through Crossing Configurations: Effect of Crossing Angles and Walking Speeds on Speed Variation and Evacuation Time. *Sustainability* **2022**, *14*, 15366. https://doi.org/10.3390/su142215366

Academic Editors: Shuchao Cao, Xiaomeng Shi and Mohcine Chraibi

Received: 27 October 2022
Accepted: 16 November 2022
Published: 18 November 2022

1. Introduction

Studies on complex pedestrian movements could be useful for the safe and efficient design of pedestrian facilities in both indoor and outdoor spaces [1,2]. This is significant as crowd disasters have become more frequent and are larger in scale due to an increase in the number of mega-events and walkable infrastructure [3]. However, these disasters are often caused by the inappropriate utilization of space and the systemic failure of organizations to provide safe pedestrian facilities. A well-designed pedestrian facility together with proper management strategies can provide an efficient flow of pedestrians, as well as safe evacuation in case of emergencies [3–5]. As walking facilities are critical components of sustainable transportation systems, the efficient and effective design of pedestrian facilities helps to promote this mode of active transport. This also plays a vital role in improving the quality of life by reducing the use of motorized modes of transport [6]. However, the design of safe and efficient pedestrian facilities requires insight into complex human movements such as intersecting pedestrian streams for varying speed conditions.

Assessing safety and collecting data for highly complex human behaviors, which are continuous in movement space, is challenging [7,8]. These data can be obtained either from experimental methods (e.g., crowd experiments using animals and social insects, controlled laboratory experiments with human crowds, virtual reality (VR) and augmented reality (AR)-based crowd experiments, hypothetical choice surveys, and evacuation drills) or from field methods, including post-incident analysis of real incidents, field observations in natural settings, or qualitative interviews [8]. Animal and insect experiments are advantageous for panic situations that cannot be performed using human subjects due to ethical reasons [9–11]. However, controlled laboratory experiments with human subjects are a reasonable compromise between animal experiments and field observations. These experiments are comparatively easy to replicate and allow the researcher to control certain variables while studying the effect on others [7]. Furthermore, computational tools for the simulation and design of pedestrian facilities for evacuation largely depend on assumptions that are found to be inconsistent or unrealistic due to the lack of human and social behavioral data [12]. Therefore, experiments with human subjects are necessary for the validation of existing models for both normal conditions, as well as in situations where pedestrians move at higher speeds than in normal walking conditions.

Studies on interactions of pedestrian crowds with different geometrical settings, such as, turning, merging, and intersecting pedestrian streams, are of particular interest as they are very common features in pedestrian facilities. These movements require collision avoidance of pedestrians with both moving and stationary obstacles. Collision avoidance with moving obstacles in the case of intersecting streams of pedestrians requires stopping or steering maneuvers, both of which affect the individual pedestrian speed considerably [13]. Numerous experimental studies have been conducted for common geometrical settings, e.g., turning [14–17], crossing [6,18,19], and merging [14,20–22] configurations, under normal, as well as evacuation, conditions. Some studies have been conducted under panic conditions using insects [10,11,23,24] and animals [25–27]. Different geometrical settings and desired speed levels can cause different bottleneck effects that can be assessed both qualitatively and quantitatively.

Previous studies have mainly focused on the bottleneck effect and capacity issues associated with these different geometrical settings. Very few studies, e.g., Lian et al. [19] and Ye et al. [17], presented the speed distributions within the congested area. However, a comprehensive characterization of speed variations within the bottleneck area has not been presented. A comprehensive microscopic evaluation of the speed distributions over the bottleneck area could be useful in identifying the mechanism of the occurrence of the congestion associated with complex geometrical settings. To address such gaps in the current knowledge, this study aims to examine the variation of velocities over the walking space and evacuation times (time-to-target) for crossing configurations of three crossing angles, under two desired speed levels. The two speed levels (normal-speed walking and slow-speed running) are used to mimic the normal and emergency evacuations, respectively. However, the speed was limited to slow-speed running to ensure the safety of the participants during the experiment. The present study is based on the controlled laboratory experimental data using human subjects collected in 2016 by Aghabayk et al. [28], which examines the influence of intersecting angles on pedestrian crowd flow using the aggregate values of the flow rate, speed, evacuation time, and travel time. The present paper provides further in-depth and microscopic analysis of the data to understand the spatial variations in speed within the corridor for intersecting pedestrian streams at varying speed levels.

This paper is organized as follows: Section 2 of the paper discusses the available empirical studies on crossing or intersecting pedestrian flows. Section 3 provides a detailed description of the experimental setup and the analysis methods. Qualitative, as well as quantitative, discussions on the results are provided in Section 4. Finally, in Section 5, the conclusions are presented.

2. Related Works

Various influencing factors, such as flow ratio, boundary conditions, the width of the walking facility, intersecting angles, and human factors (collective, as well as individual) have been studied in the past to provide insight into the characteristics of intersecting pedestrian flows using laboratory experiments. The first human subject-based experiments for intersecting pedestrian streams were carried out in the Netherlands by Dameen and Hoogendoorn [29]. They experimented with 90° and 180° angled crossings with single entries and multiple entries for varying flow ratios. They identified process variables such as free-flow speed, walking direction, density, and bottlenecks to comprehensively describe the movement of pedestrians.

Helbing et al. [3] reported an experiment considering a 90° intersecting scenario and then simulated such behaviors using the social force model [30]. They found that there were lane formations in intersecting regions and these lanes or stripes were formed at an angle of 45° for the intersection of two unidirectional flows. Similar observations regarding diagonal pattern formation were also made by Hoogendoorn and Daamen [31] for crossing movements. However, the intersection of three or more pedestrian streams produced short-lived patterns, including rotary traffic in clockwise or counterclockwise directions, dominant pedestrian flow in one direction with the other direction clogged, stripe formation, and blockages [3]. The formation of a dominant pedestrian flow in one direction with the other direction being clogged was also observed in the experiments conducted by Dias et al. [11] using ants under an induced panic situation. Nevertheless, the other patterns, e.g., diagonal stripes, were not observed in intersecting streams of ants. Recently, a quantitative analysis of the stripe formation in the intersection area concerning density conditions was provided by Zanlungo et al. [32]. Mullick et al. [33] introduced computational methods to analyze the striped patterns, in addition to analyzing the geometric properties of the stripes. Bode et al. [34] found that, in four-way intersecting streams, the relative dominance of the streams can switch stochastically, and the jams in some streams can coincide with higher flow rates in other streams. Helbing et al. [3] also proposed improvements for the intersection of two bidirectional flow configurations of pedestrian flow by providing obstacles in the center of the junction.

The headway–speed relationship for intersecting flows with a crossing angle of 90° and a flow ratio of 50:50 was investigated by Asano et al. [18] in Japan. The tendency of decreasing average speeds in small headways was found to be statistically not significant. Crossing configurations of 45°, 90°, 135°, and 180° were also used and the speed–density relationship at the crossing point was also explored in this study. They found that for 90° and 135° scenarios, even for lower flow levels, the speeds of pedestrians were affected by the crossing angles. Wong et al. [6] proposed a pedestrian stream model for crossing pedestrian flows using the data collected from a controlled experiment. In the experiment, they considered four crossing angles, i.e., 45°, 90°, 135°, and 180°. They explained that the capacity decreases with an increase in the crossing angle. The outcomes of this study further explained that the rate of speed reduction is greater when the intersection angle increases from 0° to 90°; however, the rate of speed reduction became lower when the angle exceeds 90°. Versluis [35] studied the interaction between intersecting pedestrians at a microscopic level, i.e., person-to-person and person-to-small group interactions. The study mainly focused on 0°, 45°, 90°, 135°, and 180° crossing scenarios. Individual pedestrians performed interaction movements in 88% of cases. Moreover, men were found to have a strong preference for passing through the right-hand side when compared to women.

Comparing the speed–density relationships for 90° and 180° intersections in varying conditions for blocked and unblocked sides, Zhang and Seyfried [36] concluded that the intersection angle has no impact on the fundamental diagrams, at least for these angles. As they explained, the collision avoidance patterns are not influenced by the intersection angle and this may be the reason for the above observation.

The characteristics of oblique pedestrian streams were studied by Sun et al. [37] quantitatively and qualitatively by varying the pedestrian volume levels and intersecting angles. A total of five intersection angles, i.e., 30°, 60°, 90°, 120°, and 150°, were considered in this study and showed that, for low flow rates, 30° was more efficient compared to the other angles. They further explained that the distance moved by individual pedestrians before initiating the crossing maneuver increased with an increase in flow due to less availability of gaps. Cao et al. [38] compared the pedestrian fundamental diagrams from China and Germany. The fundamental diagrams showed a considerable difference, which is attributed to the difference in average body dimensions of Westerners and Asians, motivation, and competitiveness of participants in these experiments. Lian et al. [19] explored four-directional intersecting pedestrian flows for 90° crossing configurations using the data collected through a controlled experiment. The results from this study indicate that the local density at the middle of the intersection could reach up to 10 peds/m^2 and the densities decrease towards the corridors. The speeds and flows of this study were consistent with the speeds reported by Helbing et al. [39] for the local densities of less than 5 peds/m^2. However, when the local density exceeded 5 peds/m^2, flows and speeds were higher in Lian et al. [19].

Controlled laboratory experiments have been conducted in the past for intersecting flows using animal subjects, representing the panic situation that cannot be done using human subjects due to ethical and safety reasons [40]. Being a non-invasive method, using non-human biological entities may provide insight into human collective behaviors. Dias et al. [11] conducted controlled experiments using ants to investigate crossing behaviors in a panic situation. One of the main observations in this study was that one stream is blocked, while the other stream moves forward, i.e., there is a transition of the clogging and shockwave between the two streams. The clogging period was observed to be unsymmetrical, with substantial variations in the two streams. This phenomenon, if arising in intersecting corridors of pedestrians, could pose a dangerous situation wherein the crowd forces could increase to unacceptable levels.

Aghabayk et al. [28] investigated the impact of intersection angles and desired speed on the outflow rate and evacuation time of crossing configurations using the data collected through a controlled experiment. The paper considered three intersection angles, i.e., 30°, 90°, and 150°, and two desired speed levels, i.e., normal-speed walking and jogging. Such crossing configurations can be observed in numerous real-world situations, such as commuters intersecting each other in train/metro stations or crossing on sidewalks or intersections. They used a deviation of 30° from straight movement and straight bilateral movement for their study. This choice of angle also helps in providing a comparison with the existing literature. Furthermore, as the intersection angle rises from 90° to 180°, the area of potential conflict increases, and the conflict area is least for 90°. Therefore, it is essential to understand the effects of both acute and obtuse angles. The outcomes of this study indicate that a 30° intersection is the most efficient configuration compared to 90° and 150°, as a 30° intersection displayed higher flow rates and lower delays for both speed levels. Furthermore, for normal-speed walking cases, the walking speed steadily decreased with the increasing intersection angle. In contrast, for jogging cases, a 7% increase in average walking speed was noted when the angle was increased from 90° to 150°. As described in this study, this increment might be due to the agitation of pedestrians who were stuck at the junction. That is, after passing the congested region, the pedestrians tend to regain speed faster.

It can be noted that a wide range of intersecting angles under varying flow ratios and desired speed levels have been considered in previous studies to explore pedestrian behaviors at crossing configurations. These studies generally examined average speeds and flows, as well as the capacity of crossing configurations. Very few studies, e.g., Lian et al. [19], presented the distribution of the densities within the bottleneck area of the intersection. However, detailed evaluations of the characteristics of the distribution of the congestion have not been provided. To identify the congestion occurrence mechanism and bottleneck effect associated with complex geometrical settings, detailed examinations of the distribution of speeds and densities under different walking conditions are necessary. Understanding the bottleneck effect and congestion mechanisms is critical for the safe and efficient design of pedestrian facilities, especially to avoid undesirable situations such as stampedes. Considering such applications, this study uses the data collected through the controlled experiment by Aghabayk et al. [28], which considered three intersection configurations (30°, 90°, and 150° intersection angles) and two desired speed levels (normal-speed walking and jogging) to comprehensively investigate the spatial variation of individual speeds and delays. The details of the experiment and the analysis methods are discussed in the next section.

3. Methods

3.1. Controlled Experiment and Trajectory Data

A controlled laboratory experiment was conducted at the University of Tehran, in November 2016, with 89 participants (62 males and 27 females). The age of the participants in this experiment ranged from 13 to 84 years. Three intersecting angles, i.e., 30°, 90°, and 150°, were considered for the experiment. For each angle setup, the pedestrians were divided into two groups of equal numbers. The experiments were conducted under two speed conditions, i.e., normal-speed walking and slow-speed running or jogging. During normal-speed walking scenarios, experiment participants were instructed to walk at their normal walking speed, and during slow-running scenarios, the pedestrians were asked to jog or run slowly through the experiment configurations. Each of the normal walking and jogging conditions was repeated three times, making 18 total experiments for the unblocked condition (3 angles × 2 walking speeds × 3 repetitions). The participants were stationed randomly in the two intersecting groups to eliminate any bias and to prevent the participants from learning the movement strategies while the experiments were being repeated.

The intersecting walkways were created using tapes and traffic cones. Each walkway had a uniform width of 1.5 m with a minimum length of 8 m. The width of the walkway was just enough to allow a maximum of three participants to walk/jog side by side. For better visibility during data extraction, 44 participants (Group 1) were given white hats and 45 participants (Group 2) were given blue hats. The entire experiment was filmed using a crane-mounted camera placed exactly above the center point of the junction at a height of 8 m. The video was recorded with 25 frames per second in Full HD quality. Figure 1 shows the trajectories and screenshots obtained for the three intersection angle scenarios. The collected trajectory dataset was used in the present study to explore the spatial distribution of speeds and time to target for different crossing angles under two evacuation speeds.

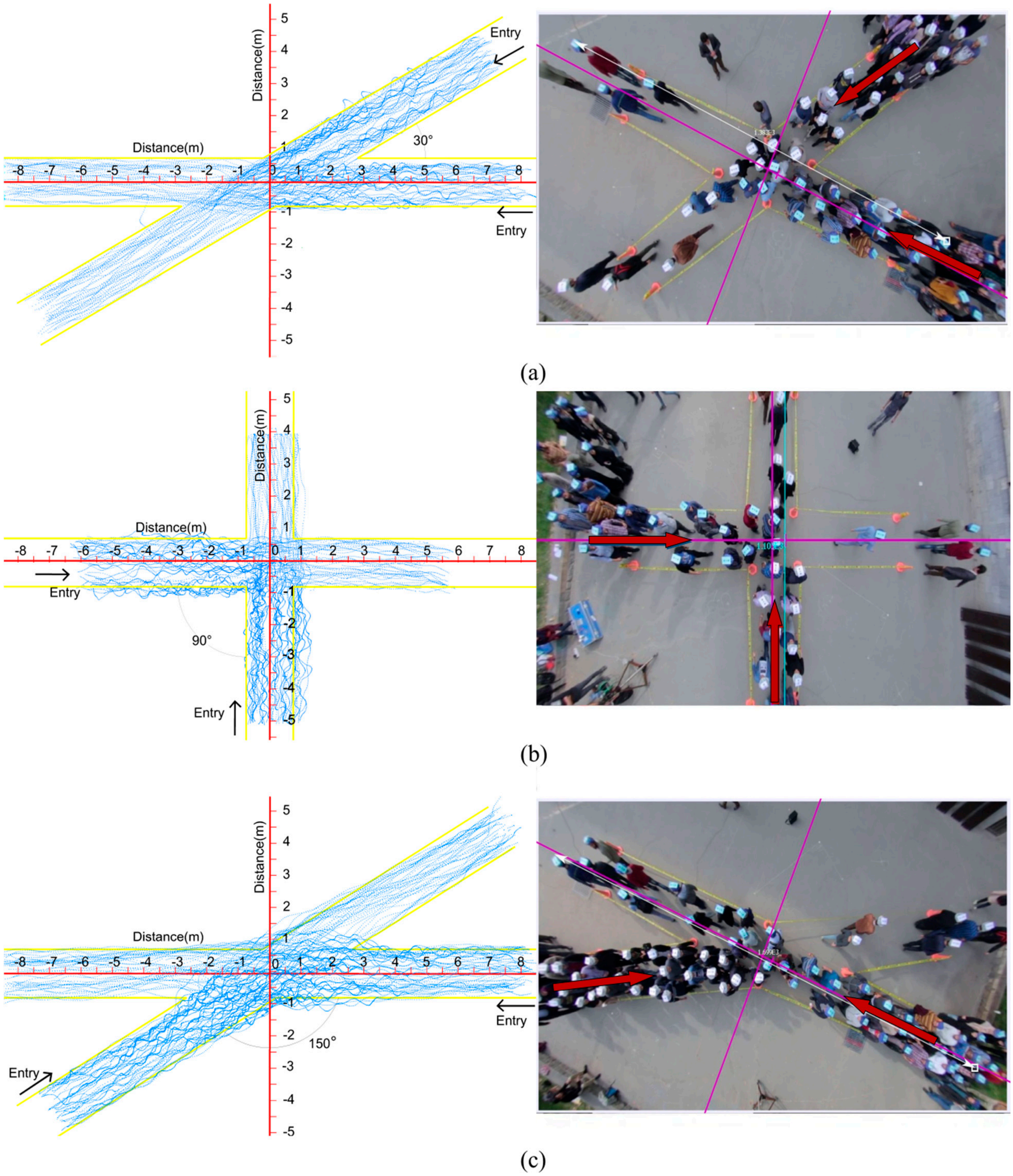

Figure 1. Trajectories and screenshots of pedestrian experiments for walking scenarios: (**a**) 30°, (**b**) 90°, and (**c**) 150° (redrawn from Aghabayk et al. [28]).

3.2. Analysis Methods

The trajectories were extracted from the recorded video footage using video tracking software (Tracker®). The extracted trajectory data consisted of the location (x, y coordinates) of each participant at every 0.04 s time interval. The raw data that consisted of trajectory points (x and y coordinates) at every 0.04 s were imported to MATLAB for further analysis. The speeds were averaged for every 5th time frame for each participant to obtain the average speed at each location. The average speed was plotted for all scenarios and directions (direction 1 and direction 2) for each of the three experimental trials. It was noted that the trends were similar for each of the six conditions for all the scenarios except for two conditions (90° jogging—trial 2—direction 1 and 150° jogging—trial 3—direction 2). The 90° jogging—trial 2—direction 1 showed a sharp decrease in speed followed by a short length of congestion and the 150° jogging—trial 3—direction 2 showed a drastic reduction in speed very close to the starting point of the trial, followed by a very flat and prolonged area of congestion. Such trials that deviated significantly from other trials were omitted from the rest of the analysis. The average speeds were plotted for each angle and for the different speed levels to analyze the effect of angle and desired speed on the spatial distribution of instantaneous speeds. Different colors were used to show distinct speed ranges using the MATLAB plot function.

The trajectories (x, y) for all the six scenarios (3 angles × 2-speed levels) at every 0.04 s were plotted against instantaneous velocity (v) using MATLAB software. Further analysis of spatial variation of speed was carried out using the instantaneous speeds throughout the corridor. Robust-LOESS (LOcally Estimated Scatterplot Smoothing) was used to estimate the smoothed or average speed profiles. The RLOESS method uses a locally weighted linear regression to smooth data by applying a quadratic polynomial. It is considered local, as the smoothed value is defined by nearby data points within the specified span. The robust function is a weight function that makes this process resistant to outliers. The unpaired two-sample *t*-tests were conducted to statistically compare the average minimum speeds for different angles and speeds.

The heat maps were generated using MATLAB software for the x, y, and v values for all the angles and the different walking conditions adopted in the study. The heat maps were generated using a mesh size of 250 points and the data mean was filtered around 15 points in four directions (top, bottom, left, and right). Qualitative analysis was performed using the above-mentioned heat maps to identify the critical locations at the intersection and corridors where the speed variation is significant.

To analyze the lateral variation of speed, the corridors were divided into three lanes (inner, middle, and outer lanes) of 0.5 m width for each of the six scenarios. The variation of speed in each of the lanes was plotted against distance for comparing the differences. Furthermore, the space utilization of the walkway and the intersection was analyzed by using heat maps of the probability of the trajectory points. A time-to-target analysis was also carried out to estimate the delay caused to the pedestrians due to intersecting streams of pedestrians and the resulting congestion. The distance versus the time taken to complete the trajectory of individual pedestrians was used for this analysis.

4. Results and Discussion

4.1. Spatial Analysis of Instantaneous Speeds

Figure 2 shows the trajectory data point of each pedestrian for each of the scenarios, plotted for the two considered speed levels. The variation in color shows the variation of instantaneous speed for each trajectory point ranging from 0 m/s to 5 m/s. Extremely low velocities (0 m/s to 0.5 m/s) are represented by black and higher velocities (>3.5 m/s), as in the case of jogging, are represented by blue.

The boundaries for the experimental setup were demarcated using tapes and cones, and, as a result, the participants tend to deviate slightly from the marked path when there is an increase in congestion. This deviation is higher for the jogging scenarios. This could be due to a similar phenomenon as that observed by Sun et al. [37] for varying flow conditions, where, for higher angles and higher flow conditions, participants tend to slow down or stop at the intersection for gaps to cross and also walk for more distance before crossing. Therefore, with higher congestion and a larger reduction speed, the participants tend to deviate more from the marked pathway if the boundaries are not rigid. This could also be critical in conditions with walkways restricted by solid or rigid edges that would prevent pedestrians from moving in a lateral direction while trying to move forward. That is, such locations could create congestion and stampedes. Hoogendoorn et al. stated that pedestrians generally refrain from changing directions and resort to reducing the speed during crossing movements as the disutility of changing directions is greater than the disutility of reducing speed [31]. However, in the present study with no rigid or solid edges, the pedestrians tend to reduce speed, as well as change direction, in areas closer to the intersection. Lian et al. also reported that the average speed decreased quickly in the intersection area at the beginning of the experiment, which is consistent with the results of this study [19]. However, Lian et al. [19] reported the results for time, while we used the spatial analysis for the intersection. Moreover, Lian et al. [19] also reported the deviation in the path of the pedestrians as the congestion increased.

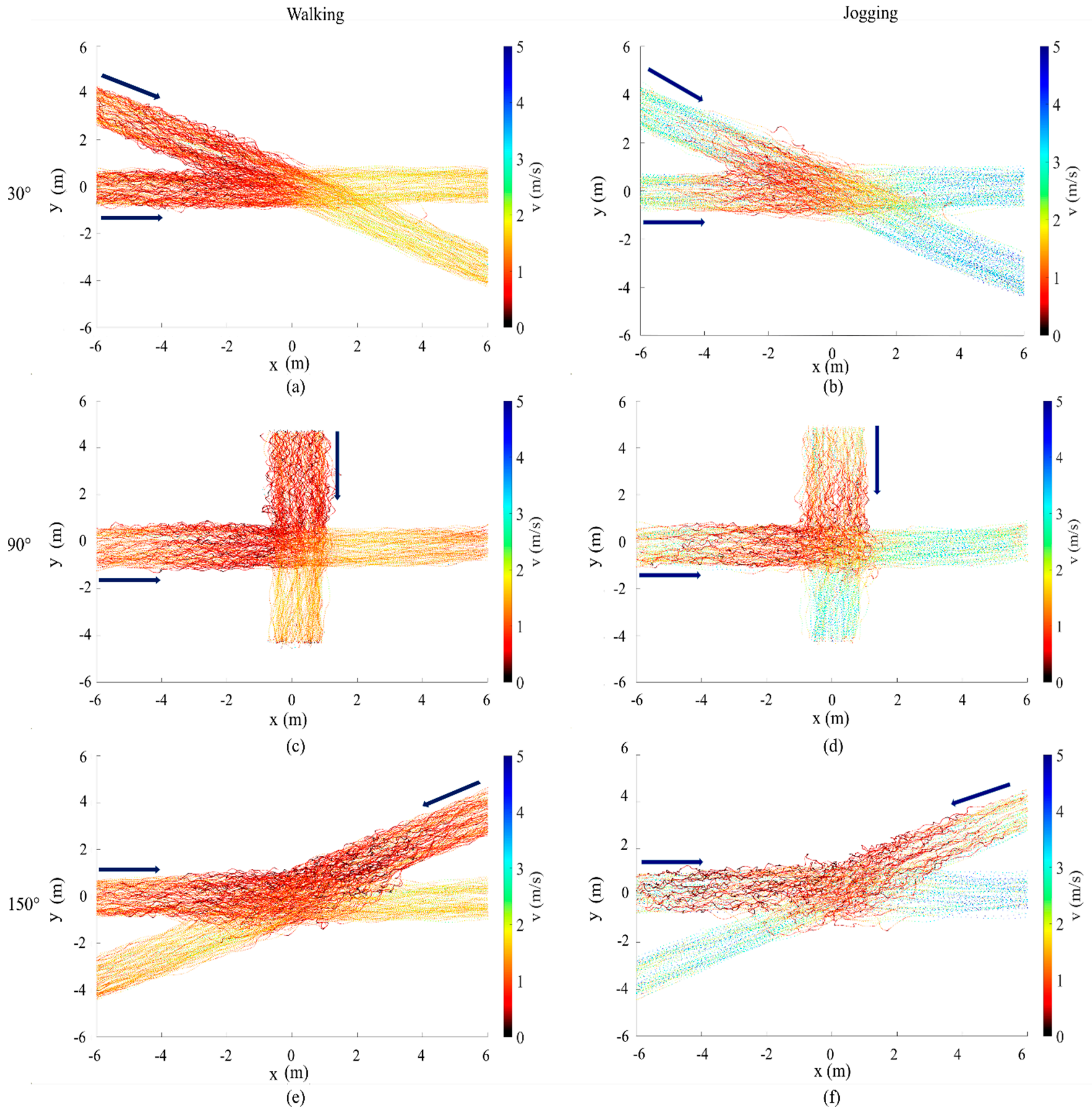

Figure 2. Trajectories of pedestrian experiment with instantaneous speeds for: (**a**,**b**) 30°, (**c**,**d**) 90°, and (**e**,**f**) 150° for walking and jogging scenarios.

Smaller and zero velocities are represented by black in Figure 2. This congestion situation is also characterized by highly fluctuating trajectories, as pedestrians have higher body deflections due to congestion [41]. For all the walking scenarios, the low-velocity fluctuating trajectories extend to the start point. However, for jogging scenarios, the low-velocity fluctuating trajectories are the least for smaller angles (e.g., 30°) and the highest for large angles (e.g., 150°). This implies that the flow of participants was faster for higher desired speeds and smaller intersection angles. This is in line with the observations in Ren et al. [41], i.e., walking scenarios are more likely to exhibit higher fluctuations than running scenarios.

4.2. Analysis of Average Speeds

Figure 3 shows the variation of average speeds along the corridor for the six scenarios explained in Section 3.2. In this figure, the coordinate (0, 0) at the center of the intersection is shown as 0 m. The instantaneous speed data points were averaged using the moving average method. As can be seen from Figure 3, the speed variation (or scatter) along the corridor is lower for the walking cases compared to the jogging cases. The jogging conditions are also characterized by a higher reduction in speed, i.e., higher decelerations, compared to walking cases when approaching the intersection. For all cases, the minimum speed occurred at an upstream location of the junction, indicating that the congestion tends to occur approximately 1–2 m before the middle of the intersection. In contrast, according to the outcomes, i.e., density distributions, of the study by Lian et al. [19], the congestion occurred in the middle of the intersection. The dimensions of the corridors (i.e., width = 3.2 m) and the experiment conditions (i.e., four directional crossing scenarios) in Lian et al. [19] were different, and, therefore, different outcomes can be expected.

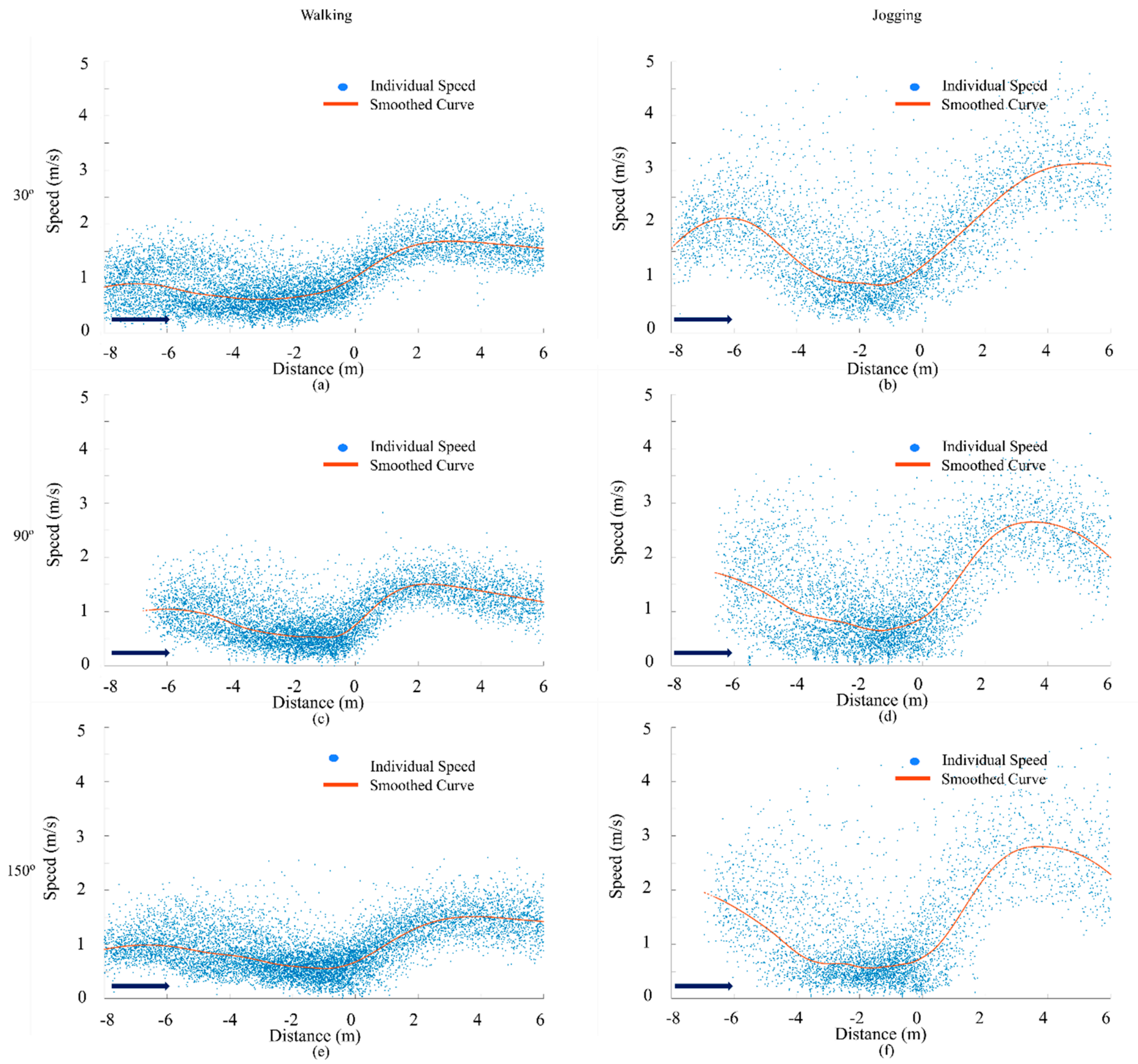

Figure 3. (**a**–**f**) Speed profiles along the corridors for different intersection angles and desired speed conditions (the smoothing was done using the RLOESS method with alpha value = 0.3).

From the dataset associated with the graphs, the average initial speed, location of the onset of speed reduction, average minimum speed, location of average minimum speed, and average receding speed were extracted. The initial speed is the maximum attained average speed at the start of the experiment before the onset of speed reduction due to the impact of the intersection, and its location is termed the location of the onset of speed reduction. The average minimum speed is the speed at the lowest point on the graph after which the speed starts to increase gradually until the average receding speed is attained.

Figure 4 compares minimum speeds for all intersection angles and speed levels, with the error bars indicating the standard deviation of the average minimum speed values. The average minimum speed was observed to be higher for the 30° angle for both the walking and jogging conditions, which indicates that the speed reduction is lower for the 30° angle. This implies that smaller intersection angles cause lower speed reductions when compared to larger angles. This observation is in line with the findings by Sun et al. [37] for normal walking speeds, who stated that, at smaller angles, the pedestrian streams do not cross each other immediately but rather move forward to find a suitable gap to cross without a very large speed reduction. Furthermore, Sun et al. reported that, for lower flow rates, the smaller time mean speed points are lower for the 30° intersection [37]. It can be noted that, for jogging scenarios, the minimum speed is decreased with the increasing intersection angle. However, for walking cases, the minimum speed of 150° is slightly higher than the minimum speed of 90°.

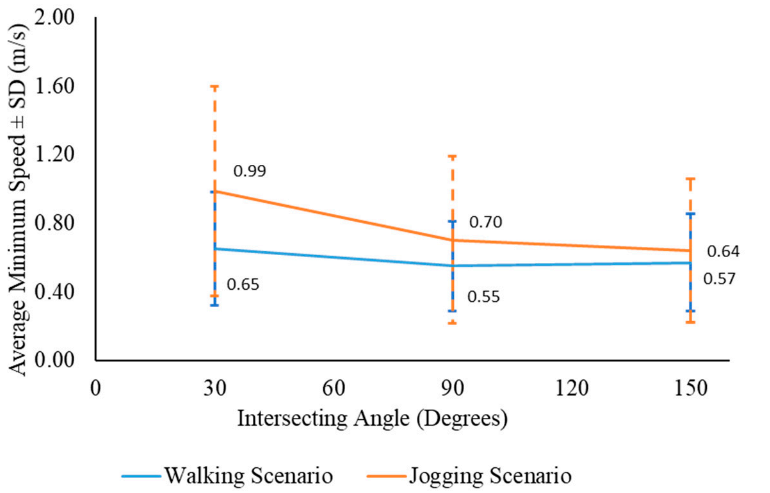

Figure 4. Comparison of average minimum speeds (±Standard Deviation) for 30°, 90°, and 150° intersections for walking and jogging conditions. (The numbers represent the minimum of the moving average speeds).

Table 1 statistically compares the minimum speeds for different angles and speed levels. An unpaired two-sample *t*-test was used to compare the average minimum speeds of the different angles of the walking and jogging scenarios. The comparison provides evidence of whether the minimum speeds significantly differed from each other. The null hypothesis is that there is no significant difference between the average minimum speeds, indicating that the difference in intersecting angle does not affect the average minimum speed. This is critical, as the reduction in speed creates a bottleneck that obstructs the flow of pedestrians. The Mean 1 and Mean 2 are the minimum of the moving average speeds for the first and second angles considered for each of the *t*-tests conducted. It can be noted that there is a significant difference between the average minimum speeds for each angle for the walking and jogging conditions except for the walking scenarios for 90° and 150°.

Table 1. Statistical comparison of average minimum speeds for different scenarios.

Scenario	Mean 1 ± SD	Mean 2 ± SD	*t*-Test Outcomes (*t*-Stat, *p*-Value)
Walk (30° vs. 90°)	0.65 ± 0.33	0.55 ± 0.26	(5.273, 0.0000) **
Walk (30° vs. 150°)	0.65 ± 0.33	0.57 ± 0.26	(4.169, 0.0000) **
Walk (90° vs. 150°)	0.55 ± 0.26	0.57 ± 0.26	(1.319, 0.1874)
Jog (30° vs. 90°)	0.99 ± 0.61	0.70 ± 0.48	(8.137, 0.0000) **
Jog (30° vs. 150°)	0.99 ± 0.61	0.64 ± 0.42	(10.424, 0.000) **
Jog (90° vs. 150°)	0.70 ± 0.48	0.64 ± 0.42	(2.198, 0.0141) *

* Significant at 0.05 level, ** Significant at 0.01 level.

As can be noted from Figure 4 and Table 1, the minimum speed for 150° is slightly higher than the minimum speed for 90°, which is contrary to intuition. However, this difference is statistically not significant. Aghabayk et al. [28] analyzed the average speed values of all pedestrians (obtained by dividing the effective corridor length by the time taken to exit from entry) and indicated a better performance by the 30° intersection for both walking and jogging scenarios. The average speed decreased consistently with an increase in angle for the walking scenario, while for the jogging scenario, there was a slight increase in average speed when the angle was 150°. However, for the present study, the analysis of minimum speeds showed that, for walking cases, the minimum speed of 150° is slightly higher than the minimum speed of 90°, even though this is not statistically significant. Wong et al. [6] noted that the speed reduction for the walking conditions of intersecting pedestrians is greater until 90°, after which, for an increase in angle, the speed reduction is offset by the lane formation. Therefore, the rise in minimum speed for an increase in angle for the walking scenario could be due to the lane formation effect, as explained by Wong et al. [6].

The minimum speeds were statistically compared with the average receding speeds for each angle and speed level, as summarized in Table 2. An unpaired two-sample *t*-test was used to compare the average minimum speeds and average receding speeds of the same angles for all the scenarios. The comparison provides evidence of whether the minimum speeds significantly differed from the receding speed in each scenario. The null hypothesis is that there is no significant difference between the average minimum speed and receding speed, indicating that the intersecting angle does not affect the average speed for the scenario. If the reduction in speed is significant, then it creates a bottleneck near the intersecting area, which obstructs the flow of pedestrians. The results indicate that the speed reduction was significant compared to the average receding speeds for all cases. The percentage reduction in speed is less for 30° for both walking (60.84%) and jogging (68.68%) conditions, which indicates that 30° intersections outperform all other intersections.

Table 2. Statistical comparison of average minimum speed and receding speed for different scenarios.

Scenario	Average Minimum Speed ± SD	Average Receding Speed ± SD	*t*-Test Outcomes (*t*-Stat, *p*-Value)
Walk (30°)	0.65 ± 0.33	1.70 ± 0.27	(54.896, 0.00) *
Walk (90°)	0.55 ± 0.26	1.50 ± 0.25	(59.065, 0.00) *
Walk (150°)	0.57 ± 0.26	1.52 ± 0.28	(55.316, 0.00) *
Jog (30°)	0.99 ± 0.61	3.15 ± 0.67	(53.432, 0.00) *
Jog (90°)	0.70 ± 0.48	2.59 ± 0.50	(60.824, 0.00) *
Jog (150°)	0.64 ± 0.42	2.71 ± 0.68	(57.892, 0.00) *

* Significant at 0.01 level.

From Tables 1 and 2, it can be noted that the minimum speeds and receding speeds are higher for the jogging cases compared to the walking cases, even though the percentage speed reductions are higher for the jogging cases. Previous studies have demonstrated that clogging and, as a result, delays could occur when the desired speeds are higher, and that phenomenon was called "the faster-is-slower effect" [42]. However, several studies that considered turning and merging configurations stated that the outflow rates could be higher when the receding speeds are higher [21,28]. The findings of these previous studies are in line with the current study.

4.3. Spatial Distribution of Average Instantaneous Speeds

Spatial heat maps can be used to analyze the variation in average speeds over the walkway, especially in the regions within the intersection area, by using a variation in color cues. The spatial heat maps (as shown in Figure 5) were plotted using the trajectory points (x, y) and average velocity (v) for all the scenarios.

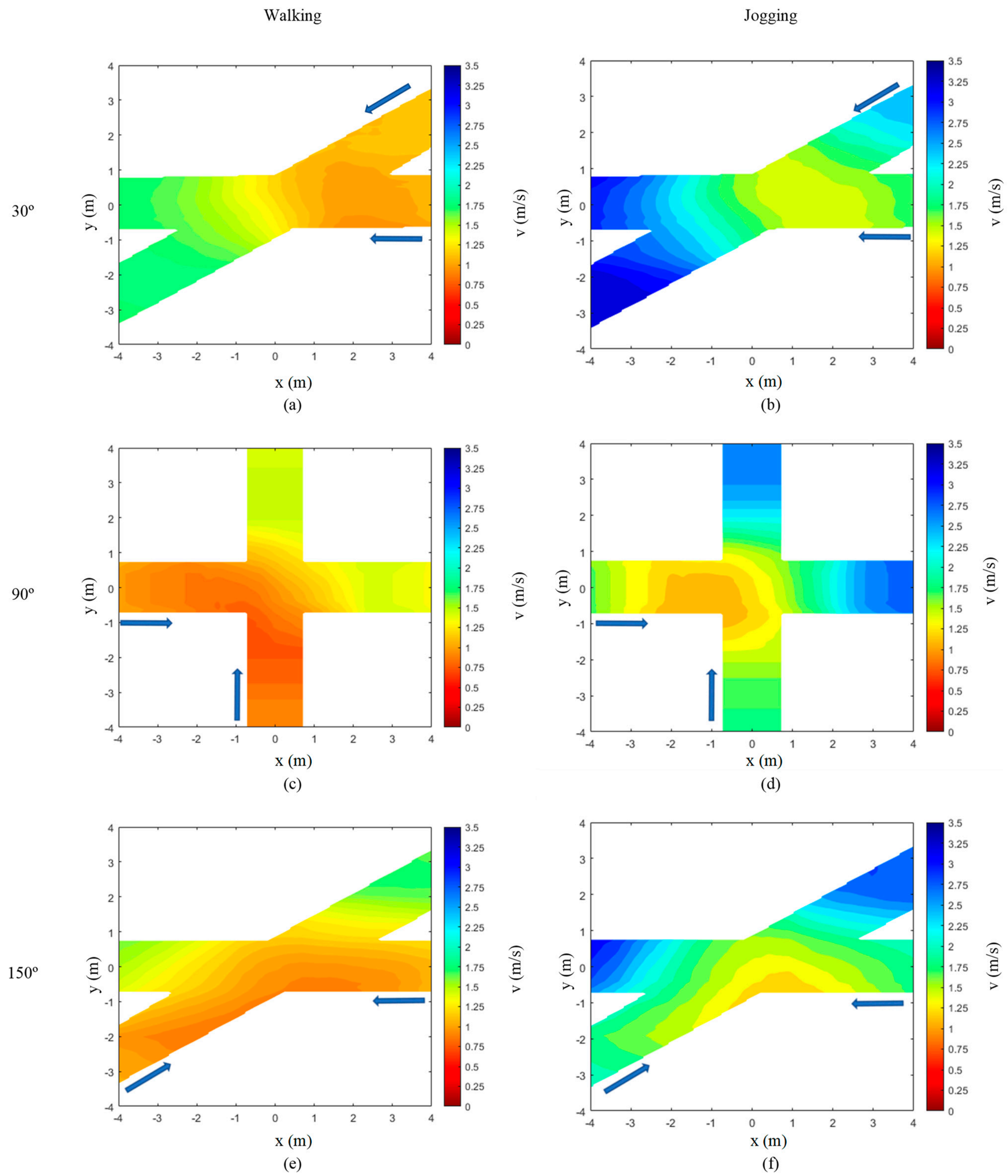

Figure 5. (**a**–**f**) Spatial distribution of speeds for different intersection angles and speed levels.

The speed values range from 0 m/s to 3.5 m/s, indicated by red and blue, respectively. The variation in the color of velocity indicates an unsymmetrical reduction in speed in the two corridors of the intersection, even though the experiment setup is geometrically symmetrical and the crowd size was the same for both streams. However, this trend varies in intensity for the different scenarios, with higher variation for lower angles in the case of the walking scenario, whereas, for the jogging scenario, the unsymmetrical nature is more predominant for the higher angles, especially the 90° intersection. This could be due to the phenomenon of leading pedestrian movement in one direction while the other direction is waiting, as reported by Helbing et al. [3]. Dias et al. [11] and Shahhoseini et al. [24] have also reported a similar phenomenon while studying the characteristics of merging crowds using panicked ants. These studies have listed the stop-and-go phenomenon in the corridors as the prime reason for the imbalance in the heat maps. However, the symmetry in velocity is regained as soon as the pedestrians reach the area where they started regaining speed. The speed reduction is severe at 90° for both walking and jogging conditions, as indicated by the higher-intensity red color in the intersecting region in these two scenarios. Moreover, it can be visualized that the congestion and resulting reduction in speed are severe in the inner corner of the intersection in all scenarios. The speed reduction for unidirectional flows is more severe in the corners, as reported by Hannun et al. [43]. Thus, for both unidirectional flow through bends, as well as the bi-directional flow of pedestrians, the speed reduction is greater at the corners or bends. This speed reduction is an important aspect that can be considered for the improvement in the design of pedestrian corridors. The shape of the inner angle can be modified to have curves or a series of smaller angles instead of sharp edges to prevent this speed reduction phenomenon while designing pedestrian facilities.

4.4. Average Speed Profiles along Corridors

In this section, the variation in speed is examined by considering the lateral distance from the intersecting stream by dividing the lateral distance of the straight stream into three equal parts of 0.5 m width virtually, as shown in Figure 6a–c. The corridor (1.5 m width) was divided into three virtual lanes of 0.5 m width, and the speeds were averaged at every 1 m. The lane configurations and the sections over which the velocities have been averaged are shown in Figure 6. Figure 7a–f shows the lane-wise variation of speed. The inner lane is defined as the one that lies adjacent to the intersecting stream of pedestrians. For all conditions, the inner lane of the intersection shows the lowest average minimum speed. The inner lane is impacted the most, as the pedestrians in this lane are obstructed by the intersecting pedestrians first. It can further be noted that the minimum average speed lies in the section between 0 m and −2 m (except for the 30° walking scenario, where the average minimum speed lies between −4 m and −2 m). For smaller angles, the speeds have less variation when comparing the inner, middle, and outer lanes. However, as the angles increases, there is a wider variation in the speed between the lanes. For 150°, as well as for 30°, the recovery of speed requires a larger distance than for 90°. Thus, while comparing the different lanes (i.e., within the corridor), speed variation is affected mainly by the angle of the intersection rather than the speed at which the pedestrians are moving. The findings are in line with those of Hannun et al. [43], who observed that the speed reduction is the lowest in the inner lanes for unidirectional flows in bends.

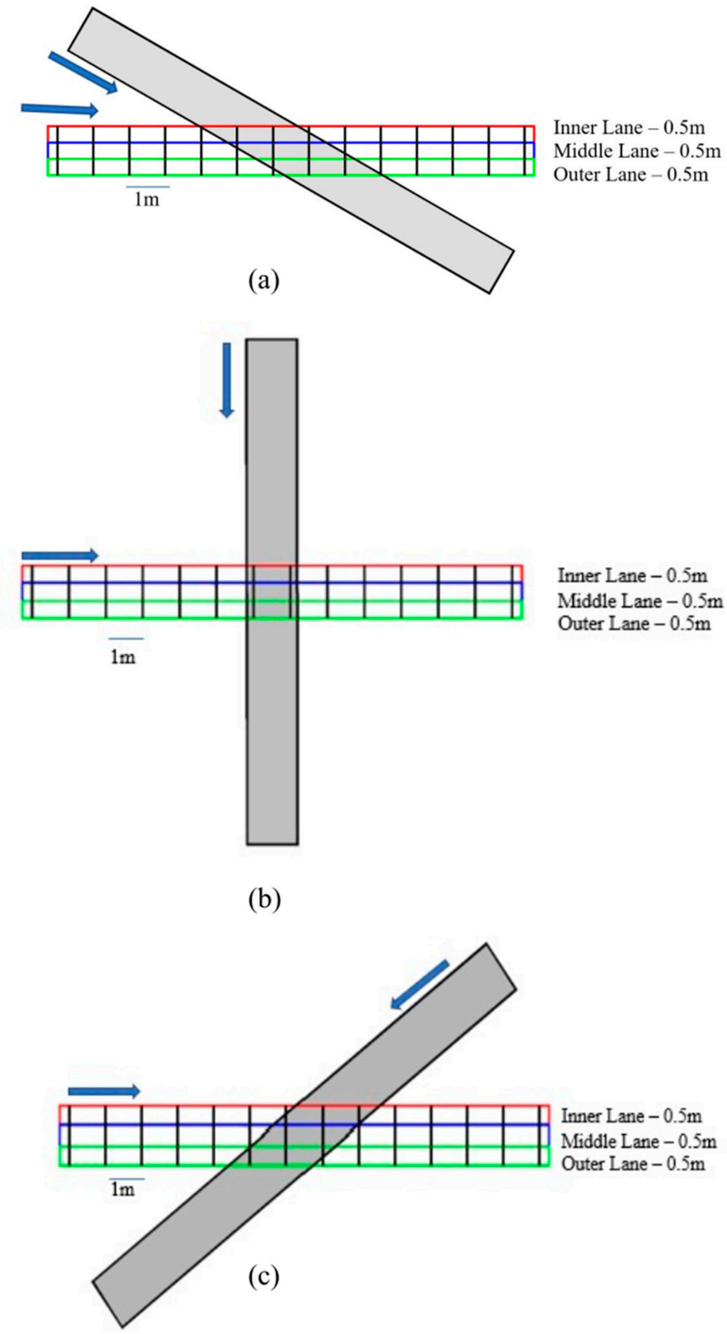

Figure 6. (**a**–**c**) Definition of lanes in the longitudinal direction. For 30°, 90°, and 150°, respectively.

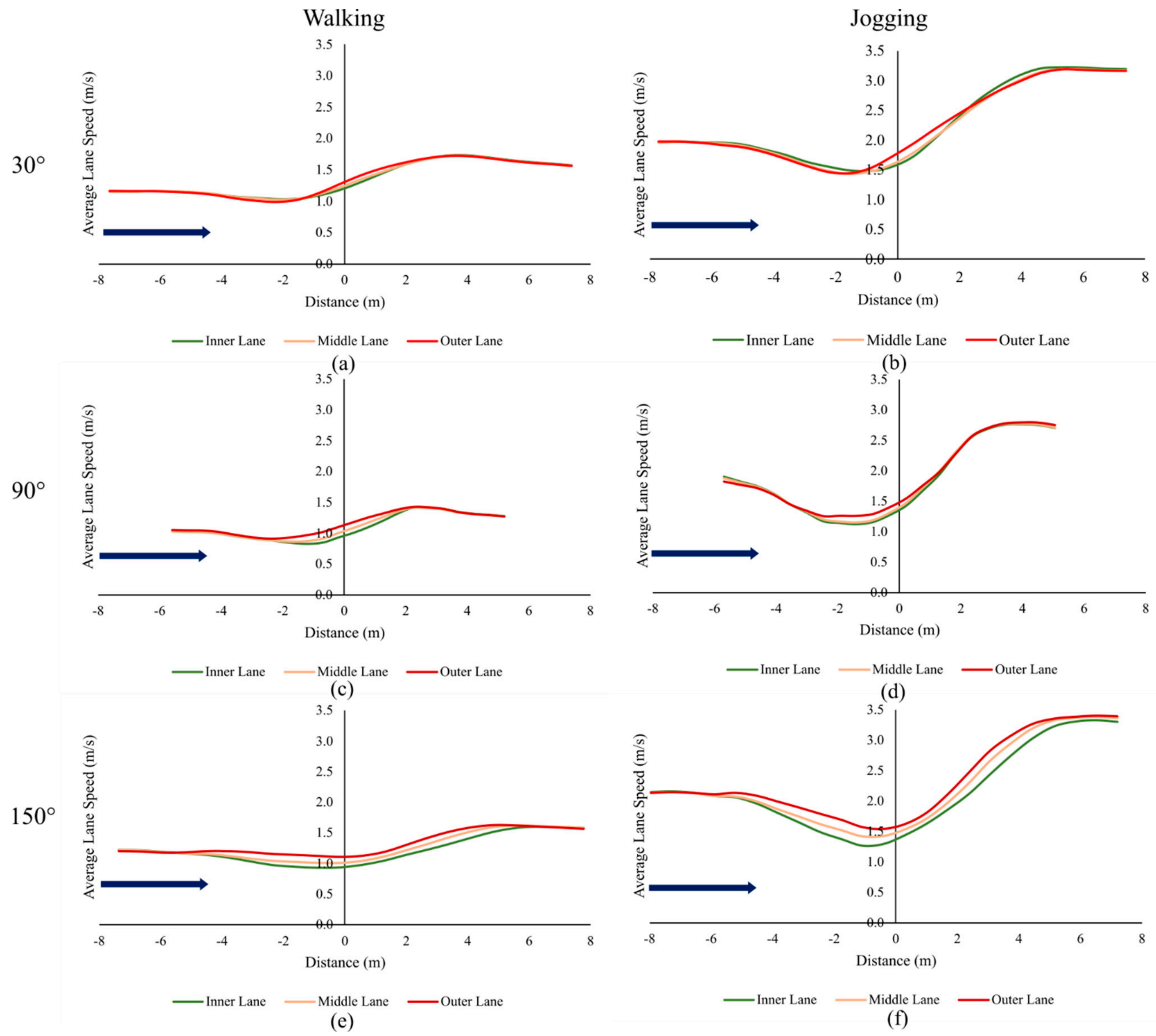

Figure 7. (**a**–**f**) Variation of speed along longitudinal lanes for different intersection angles and speed levels.

4.5. Time-to-Target Analysis

This section analyzes the speed variation with time for the intersecting stream of pedestrians by studying the constriction and waiting phases in each scenario. It shows the time required to complete the evacuation in each scenario to a point located downstream of the intersection. The slope of the trajectory indicates the variation in the speed of pedestrians and congestion. A constant slope shows free-flow movement occurring when there are no obstructions to the movement, while an increase in the slope shows that less distance is covered in more time, caused by congestion due to the intersecting stream of pedestrians. The analysis was carried out using the extracted trajectories and the time taken by each pedestrian for completing the evacuation. The evacuation is considered complete when the pedestrian crosses a distance of 4.5 m downstream from the center of the intersection. The distance for evacuation is the distance between the first point of the pedestrian trajectory, i.e., 4.5 m upstream from the center of the intersection to 4.5 m downstream from the center of the intersection. From the analysis of the receding speed in Section 4.2, it is clear that in all the scenarios the pedestrians have regained their speed at

4.5 m downstream from the center of the intersection. Thus, this point was selected as the target point for evacuation.

In this analysis, the time to target is compared between the walking and jogging conditions for each angle against the distance to the target (Figure 8a–f). The red dots indicate the total distance to the target and the total required time taken from the initial point to the target by each pedestrian. In all six scenarios, there are three visible phases. There is specifically an initial phase where the pedestrians move at a constant speed towards the intersection, followed by a waiting phase where the slope of the trajectory is steep, as the pedestrians are not able to move freely due to intersecting pedestrians, similar to the waiting and constriction phases observed by Ren et al. [41]. The waiting phase is characterized by two sub-phases caused by pedestrians who are less affected and highly affected pedestrians. The less affected pedestrians have a reduction in speed, indicated by the change in slope, but the slope is constant until they cross the intersection, after which they increase their speed to attain the desired speed. The highly impacted pedestrians have trajectories with very irregular slopes, showing large variations in speeds characterized by a frequent stop-and-go motion. The third free-flow phase occurs approximately 2.5 m from the evacuation point for all the scenarios, where there are no more intersecting pedestrians to deter the movement, and the pedestrians achieve their desired speed.

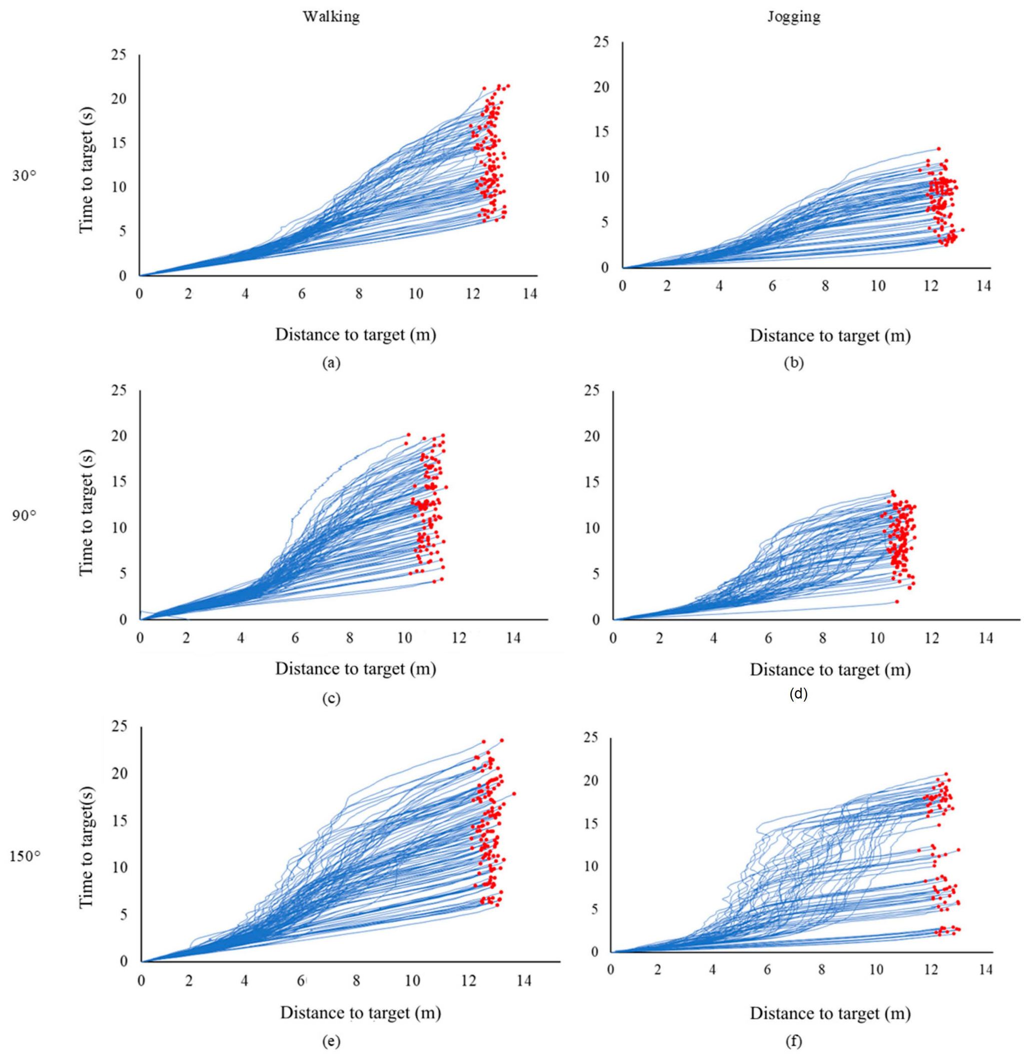

Figure 8. (**a**–**f**) Time to target vs. Distance to the target at the exit for different intersection angles and speed levels. The red dots indicate the total distance to the target and the total required time taken from the initial point to the target by each pedestrian.

Ren et al. [41] observed a lower slope for all the running scenarios compared to the walking scenarios for straight corridors. However, in the current study, due to an increase in the intersection angle, an increase in the slope can be observed when the intersection angle and desired speed increase. For the walking scenario, the slope in the waiting phase also increases, showing a gradual increase in time to target due to an increase in the angle of the intersection. The slopes for the jogging scenarios are lower for the lower intersection angles of 30° and 90°. For the 30° jogging scenario, the number of pedestrians who are highly impacted is less than in all other scenarios. However, for the jogging scenario, the slope and the time to target drastically increase as the angle of intersection increases. These observations further indicate that the decelerations become higher when the intersection angle and desired speed increase. There is a wide variation in the time to target for the pedestrians in the jogging scenario, reaching values comparable to the time required for the walking scenario for 150°, making it the least preferred intersection for both walking and jogging scenarios. Aghabayk et al. [28] observed that 30° and 90° jogging conditions had similar average travel times and would therefore perform in the same way during emergencies. However, the current study shows a wide variation in the time-to-target analysis for 30° and 90° jogging conditions. Aghabayk et al. [28] further observed that the average evacuation times widely differed in the jogging scenario for larger angles, while in the present study, the time to target varies widely across the walking passages for both walking and jogging scenarios.

4.6. Space Utilization

The utilization of the space along the corridors indicates the efficiency with which the walking facility was used during the experiment. The entire corridor and intersection area were divided into sections of 5 cm × 5 cm for all the scenarios, and the kernel density of the number of trajectory points falling in each of these sections was computed. Furthermore, the probability of the trajectory points falling in each of these sections was computed using the kernel density and was plotted for the entire section using MATLAB software (Figure 9a–f). The lower probability of space utilization is denoted by blue and the higher probability of space utilization is denoted by red. Spaces with higher congestion have a higher probability of trajectory points in that section. All the figures show lane formation before the intersection area. However, the walking scenarios showed a more evident lane formation after the intersection area. Specific lane formation cannot be identified very well for the jogging conditions after the intersection areas, except in Figure 9f. Dias et al. [44] also mentioned that the lane formations were not visible for the slow-speed running (jogging) cases for angled corridors.

The sections in the inner lanes where the pedestrian streams encounter one another are more utilized than all the other areas. Moreover, for the lower angles, the space utilization is uniform in both the incoming corridors for both walking and jogging scenarios. However, for higher angles such as 90° and 150°, the space utilization is more for one of the corridors, even though the number of pedestrians is the same for all corridors in all the scenarios. This indicates that there is more congestion in one corridor than in the other for higher intersecting angles. This can be crucial in the case of panic situations during emergencies where one of the corridors might experience more congestion than the other, even though the flow conditions in both corridors and geometrical configurations are similar.

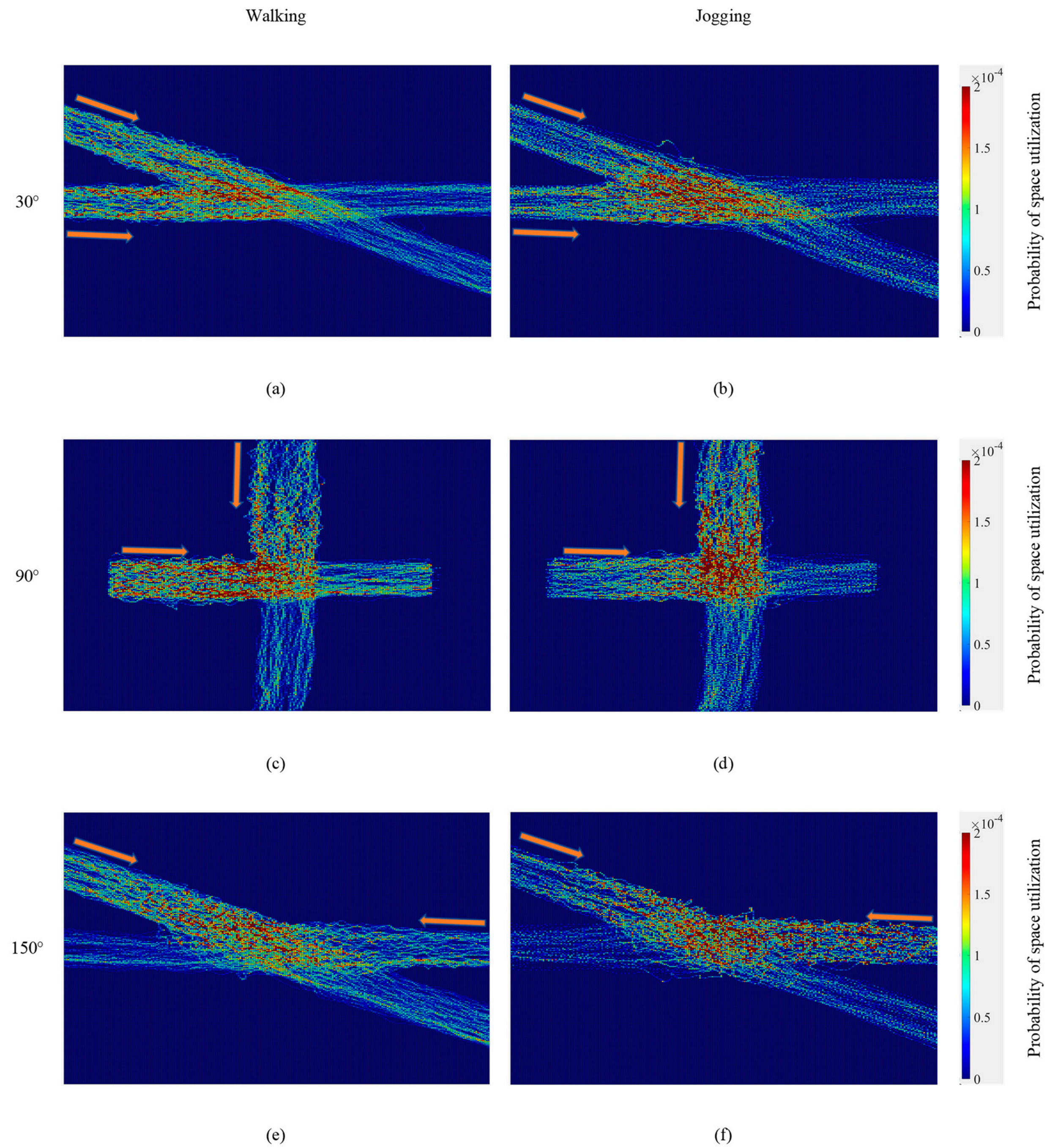

Figure 9. (**a**–**f**) Probability of space utilization for different intersection angles and speed levels.

5. Conclusions

Studies on pedestrian behaviors associated with complex geometrical settings could aid in the enhancement of pedestrian facility design to maximize the safety and efficiency of crowd flows. Furthermore, analyses of empirical data could be useful in improving pedestrian crowd modeling and simulation platforms that are commonly used to explore evacuation scenarios. In this study, the spatial variation of collective speeds, variations of the time to target, and the space utilization at crossing configurations were investigated using the trajectory data collected through a controlled experiment that considered three intersection angles, i.e., 30°, 90°, and 150°, and two desired speed levels, i.e., normal-speed walking and jogging. The comparison of average speed profiles along the corridors, minimum speeds, receding speeds, and the time to target showed that the 30° crossing configuration performed better than the 90°and 150° setups for both walking and jogging conditions.

The spatial analysis of speeds using speed heat maps and lane-based speed profiles indicated that the speed distributions along the corridors and intersection areas are not uniform and symmetric. Speeds were lower in inner lanes compared to outer lanes, indicating that stampedes could occur at the inner corners of the intersection. Furthermore, the speed distributions on the two inflow corridors were not symmetric, even though the number of pedestrians approaching the intersection from the two streams was the same and the configuration was symmetric. This could be due to the complexity and asymmetric nature of the microscopic interactions of pedestrians at crossing configurations.

The time-to-target analysis revealed that lower-angled intersections have shorter evacuation times. Although the delay for the jogging cases was lower for a given intersection angle than for the walking cases, the decelerations were greater for the jogging cases. This observation implies that stampedes are more likely to occur during emergency evacuations at higher-angled intersections. Space utilization maps revealed that, for the jogging cases, self-organized patterns might disappear, resulting in disorganized flow conditions. Such disorganized flow patterns under high-speed conditions, such as emergency evacuation, could result in stampedes, especially when the intersection angle is higher.

The findings of this study are important in understanding the congestion mechanism associated with complex crowd movements at crossing configurations, particularly under evacuation conditions. Based on this understanding, countermeasures could be devised to reduce congestion and eliminate potential stampedes at crossing configurations. The results could also help to recognize the probable location of the occurrence of stampedes in pedestrian facilities. This could assist in providing improved designs for pedestrian facilities by providing suitable intersecting angles. In addition, the trajectory data and findings of this study can aid the calibration and validation of microscopic simulation models to accurately reproduce the bottleneck effects and to evaluate different scenarios associated with crossing configurations.

In this study, a crossing configuration with narrow corridors (width = 1.5 m) was considered. Furthermore, two-way crossing scenarios were considered in the experiments. For different corridor dimensions (width) and experiment conditions (e.g., four directional flows and varying flow rates), the mechanisms of congestion occurrence and the characteristics of speed distributions may differ. Furthermore, the walking behavior of pedestrians could be affected by demographic factors and cultural influences. Therefore, such aspects should also be considered in future studies. Thus, experiments at different geographical locations with varying demographic factors (e.g., inclusion of different percentages of older and younger pedestrians) could be conducted to obtain a better understanding of pedestrian behaviors.

Author Contributions: Conceptualization, C.D. and W.A.; Methodology, C.D. and W.A.; Software, A.A.; Validation, S.S.; Formal analysis, S.S. and A.V.; Investigation, S.S., C.D. and A.A.; Data curation, K.A.; Writing—original draft, S.S. and A.V.; Writing—review & editing, S.S., C.D., W.A. and K.A.; Visualization, S.S. and A.A.; Supervision, C.D. and W.A.; Project administration, C.D. All authors have read and agreed to the published version of the manuscript.

Funding: This research received no external funding.

Informed Consent Statement: Informed consent was obtained from all subjects involved in the study.

Conflicts of Interest: The authors declare no conflict of interest.

References

1. Shi, X.; Ye, Z.; Shiwakoti, N.; Grembek, O. A state-of-the-art review on empirical data collection for external governed pedestrians complex movement. *J. Adv. Transp.* **2018**, *2018*, 1063043. [CrossRef]
2. Haghani, M. Empirical methods in pedestrian, crowd and evacuation dynamics: Part, I. Experimental methods and emerging topics. *Saf. Sci.* **2020**, *129*, 104743. [CrossRef]

3. Helbing, D.; Buzna, L.; Johansson, A.; Werner, T. Self-organized pedestrian crowd dynamics: Experiments, simulations, and design solutions. *Transp. Sci.* **2005**, *39*, 1–24. [CrossRef]
4. Gao, Z.; Qu, Y.; Li, X.; Long, J.; Huang, H.-J. Simulating the dynamic escape process in large public places. *Oper. Res.* **2014**, *62*, 1344–1357. [CrossRef]
5. Al-Ahmadi, H.M.; Reza, I.; Jamal, A.; Alhalabi, W.S.; Assi, K.J. Preparedness for mass gatherings: A simulation-based framework for flow control and management using crowd monitoring data. *Arab. J. Sci. Eng.* **2021**, *46*, 4985–4997. [CrossRef]
6. Wong, S.C.; Leung, W.; Chan, S.H.; Lam, W.H.; Yung, N.H.; Liu, C.; Zhang, P. Bidirectional pedestrian stream model with oblique intersecting angle. *J. Transp. Eng.* **2010**, *136*, 234–242. [CrossRef]
7. Haghani, M.; Sarvi, M. Crowd behaviour and motion: Empirical methods. *Transp. Res. Part B Methodol.* **2018**, *107*, 253–294. [CrossRef]
8. Haghani, M. Empirical methods in pedestrian, crowd and evacuation dynamics: Part II. Field methods and controversial topics. *Saf. Sci.* **2020**, *129*, 104760. [CrossRef]
9. Shiwakoti, N.; Sarvi, M.; Rose, G.; Burd, M. Enhancing the safety of pedestrians during emergency egress: Can we learn from biological entities? *Transp. Res. Rec.* **2009**, *2137*, 31–37. [CrossRef]
10. Shiwakoti, N.; Sarvi, M.; Rose, G.; Burd, M. Animal dynamics based approach for modeling pedestrian crowd egress under panic conditions. *Procedia Soc. Behav. Sci.* **2011**, *17*, 438–461. [CrossRef]
11. Dias, C.; Sarvi, M.; Shiwakoti, N.; Ejtemai, O.; Burd, M. Investigating collective escape behaviours in complex situations. *Saf. Sci.* **2013**, *60*, 87–94. [CrossRef]
12. Pan, X.; Han, C.S.; Dauber, K.; Law, K.H. A multi-agent based framework for the simulation of human and social behaviors during emergency evacuations. *Ai Soc.* **2007**, *22*, 113–132. [CrossRef]
13. Parisi, D.R.; Negri, P.A.; Bruno, L. Experimental characterization of collision avoidance in pedestrian dynamics. *Phys. Rev. E* **2016**, *94*, 022318. [CrossRef]
14. Zhang, J.; Klingsch, W.; Rupprecht, T.; Schadschneider, A.; Seyfried, A. Empirical study of turning and merging of pedestrian streams in T-junction. *arXiv* **2011**, arXiv:1112.5299.
15. Dias, C.; Ejtemai, O.; Sarvi, M.; Shiwakoti, N. Pedestrian walking characteristics through angled corridors: An experimental study. *Transp. Res. Rec.* **2014**, *2421*, 41–50. [CrossRef]
16. Rahman, N.; Alias, N.; Sukor, N.; Halim, H.; Gotoh, H.; Hassan, F. Trajectories and walking velocity of pedestrian walking through angled-corridors: A unidirectional scenario. In Proceedings of the IOP Conference Series: Materials Science and Engineering, Kerbala, Iraq, 4–6 November 2019; p. 012114.
17. Ye, R.; Chraibi, M.; Liu, C.; Lian, L.; Zeng, Y.; Zhang, J.; Song, W. Experimental study of pedestrian flow through right-angled corridor: Uni-and bidirectional scenarios. *J. Stat. Mech. Theory Exp.* **2019**, *2019*, 043401. [CrossRef]
18. Asano, M.; Kuwahara, M.; Tanaka, S. Multi-directional pedestrian flow model based on empirical data. In Proceedings of the 11th World Conference on Transport ResearchWorld Conference on Transport Research Society, Berkeley, CA, USA, 24–28 June 2007.
19. Lian, L.; Mai, X.; Song, W.; Richard, Y.K.K.; Wei, X.; Ma, J. An experimental study on four-directional intersecting pedestrian flows. *J. Stat. Mech. Theory Exp.* **2015**, *2015*, P08024. [CrossRef]
20. Lian, L.; Mai, X.; Song, W.; Richard, Y.K.K.; Rui, Y.; Jin, S. Pedestrian merging behavior analysis: An experimental study. *Fire Saf. J.* **2017**, *91*, 918–925. [CrossRef]
21. Shahhoseini, Z.; Sarvi, M.; Saberi, M. Pedestrian crowd dynamics in merging sections: Revisiting the "faster-is-slower" phenomenon. *Phys. A Stat. Mech. Its Appl.* **2018**, *491*, 101–111. [CrossRef]
22. Aghabayk, K.; Sarvi, M.; Ejtemai, O.; Sobhani, A. Impacts of different angles and speeds on behavior of pedestrian crowd merging. *Transp. Res. Rec.* **2015**, *2490*, 76–83. [CrossRef]
23. Soria, S.A.; Josens, R.; Parisi, D.R. Experimental evidence of the "Faster is Slower" effect in the evacuation of ants. *Saf. Sci.* **2012**, *50*, 1584–1588. [CrossRef]
24. Shahhoseini, Z.; Sarvi, M.; Saberi, M. Insights toward characteristics of merging streams of pedestrian crowds based on experiments with panicked ants. *Transp. Res. Rec.* **2016**, *2561*, 81–88. [CrossRef]
25. Pastor, J.M.; Garcimartín, A.; Gago, P.A.; Peralta, J.P.; Martín-Gómez, C.; Ferrer, L.M.; Maza, D.; Parisi, D.R.; Pugnaloni, L.A.; Zuriguel, I. Experimental proof of faster-is-slower in systems of frictional particles flowing through constrictions. *Phys. Rev. E* **2015**, *92*, 062817. [CrossRef] [PubMed]
26. Zuriguel, I.; Olivares, J.; Pastor, J.M.; Martín-Gómez, C.; Ferrer, L.M.; Ramos, J.J.; Garcimartín, A. Effect of obstacle position in the flow of sheep through a narrow door. *Phys. Rev. E* **2016**, *94*, 032302. [CrossRef]
27. Lin, P.; Ma, J.; Liu, T.Y.; Ran, T.; Si, Y.L.; Wu, F.Y.; Wang, G.Y. An experimental study of the impact of an obstacle on the escape efficiency by using mice under high competition. *Phys. A Stat. Mech. Its Appl.* **2017**, *482*, 228–242. [CrossRef]
28. Aghabayk, K.; Radmehr, K.; Shiwakoti, N. Effect of intersecting angle on pedestrian crowd flow under normal and evacuation conditions. *Sustainability* **2020**, *12*, 1301. [CrossRef]
29. Daamen, W.; Hoogendoorn, S.P. Experimental research of pedestrian walking behavior. *Transp. Res. Rec.* **2003**, *1828*, 20–30. [CrossRef]
30. Helbing, D.; Molnar, P. Social force model for pedestrian dynamics. *Phys. Rev. E* **1995**, *51*, 4282. [CrossRef]
31. Hoogendoorn, S.; Daamen, W. Self-organization in pedestrian flow. In *Traffic and Granular Flow'03*; Springer: Berlin/Heidelberg, Germany, 2005; pp. 373–382.

32. Zanlungo, F.; Feliciani, C.; Yücel, Z.; Nishinari, K.; Kanda, T. Analysis and modelling of macroscopic and microscopic dynamics of a pedestrian cross-flow. *arXiv* **2021**, arXiv:2112.12304.
33. Mullick, P.; Fontaine, S.; Appert-Rolland, C.; Olivier, A.-H.; Warren, W.H.; Pettré, J. Analysis of emergent patterns in crossing flows of pedestrians reveals an invariant of 'stripe'formation in human data. *PLOS Comput. Biol.* **2022**, *18*, e1010210. [CrossRef]
34. Bode, N.W.; Chraibi, M.; Holl, S. The emergence of macroscopic interactions between intersecting pedestrian streams. *Transp. Res. Part B Methodol.* **2019**, *119*, 197–210. [CrossRef]
35. Versluis, D. *Microscopic Interaction Behavior between Individual Pedestrians*; TU Delft Library: Delft, The Netherlands, 2010.
36. Zhang, J.; Seyfried, A. Comparison of intersecting pedestrian flows based on experiments. *Phys. A Stat. Mech. Its Appl.* **2014**, *405*, 316–325. [CrossRef]
37. Sun, L.; Gong, Q.; Hao, S.; Wang, C.; Chen, Y. Experimental study of oblique pedestrian streams. *Promet Traffic Transp.* **2018**, *30*, 151–161. [CrossRef]
38. Cao, S.; Lian, L.; Chen, M.; Yao, M.; Song, W.; Fang, Z. Investigation of difference of fundamental diagrams in pedestrian flow. *Phys. A Stat. Mech. Appl.* **2018**, *506*, 661–670. [CrossRef]
39. Helbing, D.; Johansson, A.; Al-Abideen, H.Z. Dynamics of crowd disasters: An empirical study. *Phys. Rev. E* **2007**, *75*, 046109. [CrossRef]
40. Shiwakoti, N.; Sarvi, M. Understanding pedestrian crowd panic: A review on model organisms approach. *J. Transp. Geogr.* **2013**, *26*, 12–17. [CrossRef]
41. Ren, X.; Zhang, J.; Song, W. Flows of walking and running pedestrians in a corridor through exits of different widths. *Saf. Sci.* **2021**, *133*, 105040. [CrossRef]
42. Helbing, D.; Farkas, I.; Vicsek, T. Simulating dynamical features of escape panic. *Nature* **2000**, *407*, 487–490. [CrossRef]
43. Hannun, J.; Dias, C.; Taha, A.H.; Almutairi, A.; Alhajyaseen, W.; Sarvi, M.; Al-Bosta, S. Pedestrian flow characteristics through different angled bends: Exploring the spatial variation of velocity. *PLoS ONE.* **2022**, *17*, e0264635. [CrossRef]
44. Dias, C.; Sarvi, M.; Ejtemai, O.; Burd, M. Elevated desired speed and change in desired direction: Effects on collective pedestrian flow characteristics. *Transp. Res. Rec.* **2015**, *2490*, 65–75. [CrossRef]